ACS Catalysis

Indole Photocatalysts and Secondary Amine Ligands Enable Nickel-Photoredox $C(sp^2)$–Heteroatom Couplings

Harsh P. Chavda, Kevin J. Liang, Tanner J. Megna, Olivia R. Taylor, Grace Kim, Angie L. López, and Ana Bahamonde*

Cite This: *ACS Catal.* 2025, 15, 10760−10767

ABSTRACT: Nickel-photochemical $C(sp^2)$−heteroatom coupling reactions have emerged as a powerful tool for constructing diverse molecular architectures. However, most existing methods rely on expensive photocatalysts or specialized ligands, limiting their practicality and scalability. Here, we introduce a photocatalytic initiation strategy driven by inexpensive indoles, eliminating the need for designer photocatalysts. Additionally, we demonstrate the effectiveness of highly tunable secondary amine ligands in facilitating coupling while suppressing side reactions that sequester the Ni catalyst off-cycle. Our approach enables a broad range of amination and etherification reactions with good yields and functional group tolerance, providing a scalable platform for C−N and C−O couplings that relies on a readily available photocatalyst and cost-effective, modular ligands. Finally, mechanistic investigations suggest that the reaction operates via an unconventional aryl radical-initiated Ni(I/III) catalytic cycle, distinguishing it from traditional Ni-photoredox processes. This initiation mode, in which aryl radicals are generated under mild conditions compatible with organometallic catalysis, is expected to serve as a generalizable platform for other synthetic transformations beyond Ni-catalyzed processes.

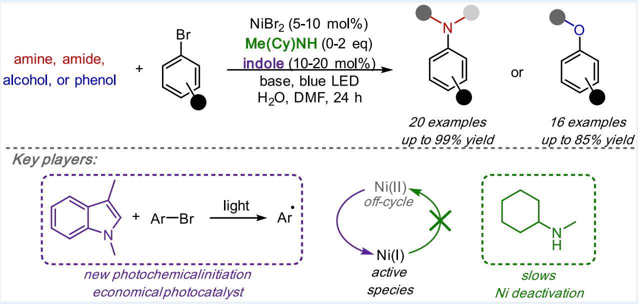

KEYWORDS: *nickel, cross-coupling, photoredox catalysis, visible light, amine, alcohol*

INTRODUCTION

Since the initial reports of Ni-photochemical aryl heteroatom couplings,[1] the field has rapidly expanded to accommodate a variety of nucleophiles, establishing itself as a valuable strategy for constructing these ubiquitous moieties.[2] Compared to traditional thermal approaches, Ni-photochemical methods typically offer broader functional group tolerance due to their mild reaction conditions and the use of softer bases. However, they still require relatively high catalyst loadings compared to state-of-the-art Pd-, Cu-, or even Ni-catalyzed processes, along with relatively expensive photocatalysts (PC).[3] As this Ni-photoredox field matured, the community has focused on circumventing the need for expensive organometallic photocatalysts.[2,4]

Central to these approaches is accessing a Ni(III) intermediate (**C**) that is prone to undergo fast C-heteroatom reductive elimination (RE) at room temperature.[5] Most reactions are facilitated by the mechanism depicted in Figure 1a and vary in the nature of the reductant used to reduce off-cycle Ni(II) species—often the resting state—back to active catalytic intermediates.[2c,6] Organic PCs[7] and chemical reductants[8] have been used as greener alternatives to organometallic PCs. However, these strategies still rely on designer PCs or present scale-up challenges due to system heterogeneity. The Baran group has also reported the use of specialized electrochemical cells as a viable alternative (Figure 1b).[9]

A more direct approach involves using UV light to photolyze off-cycle Ni(II) species, simplifying the system but at the cost of reduced functional group compatibility (Figure 1c).[10] To enable similar reactivity under visible-light irradiation, Li and Pieber have developed decorated bipyridine ligands which allow for the Ni complexes to absorb in the visible region.[11] Similarly, Xue has reported the use of a specialized Ni(0) complex to afford this reactivity with red-light irradiation.[12] Although these precedents were significant advances, they still require designer catalysts. Unfortunately, as Doyle demonstrated in 2020, the more readily available $Ni(COD)_2$ precatalyst exhibits a limited substrate scope.[13] Another viable strategy that avoids the use of PCs entirely involves using activated electrophiles, such as aryl thianthrenium salts,[14] which require additional synthetic steps, or aryl iodides,[15]

Received: May 14, 2025
Revised: May 28, 2025
Accepted: May 30, 2025

https://doi.org/10.1021/acscatal.5c03251

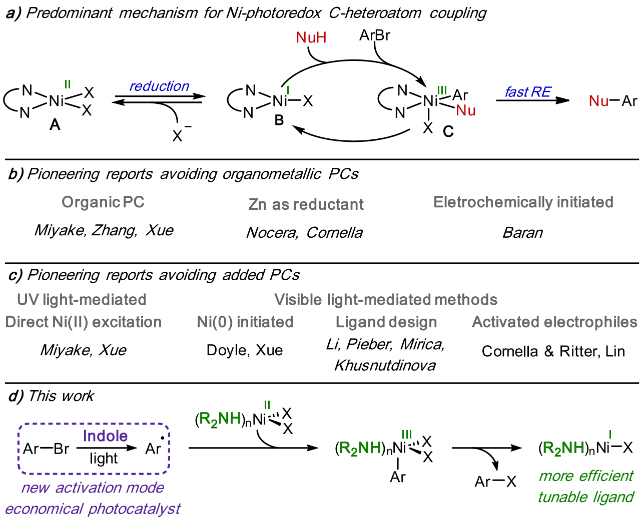

Figure 1. General mechanism and precedents for Ir-free Ni(I/III) amine and alcohol arylations.

which are less widely available than their bromide or chloride counterparts.

Notably, the majority of these methods employ bipyridine-based ligands, which have a limited structural diversity. The use of alternative scaffolds have been explored by Na and Mirica[16] and Khusnutdinova,[17] though these methodologies are currently more limited in substrate scope. Similarly, conditions with no added ligand remain restricted to specific subsets of amination reactions.[1a,8b]

In this paper, we address two major limitations: (i) the reliance on bipyridine-based ligands, which offer limited modularity; and (ii) the use of expensive Ir photocatalysts. We overcome these challenges by introducing the use of highly tunable secondary amine ligands and developing a new photocatalytic initiation driven by inexpensive indoles.

While investigating a Ni/Ir dual-catalyzed indole arylation reaction,[18] we observed that trace amounts of the indole *N*-arylated product could still be accessed in the absence of Ir. Building upon this finding, we discovered that readily accessible heterocycles, such as *N*,3-dimethylindole, could replace the costly Ir photocatalyst and enable a variety of C(sp^2)−heteroatom couplings. Furthermore, preliminary mechanistic studies revealed that indole photoinitiation operates via a rare activation pathway involving the generation of aryl radicals.

A key factor in enabling our arylation chemistry for a broad range of nucleophiles was the identification of secondary amines as suitable ligands. Concurrently with our work, König reported a Ni-photoredox strategy where *tert*-butylamine was identified as the optimal ligand for enabling C−O and C−N arylation with 4CzIPN as the organic PC.[19] However, the influence of this ligand class on the reaction mechanism was not explored. Here, we present data that highlight why amines may be privileged scaffolds for Ni(I/III) cycles. These amines are proposed to provide an optimal balance of steric hindrance to suppress side reactions while being sufficiently electron-rich to promote turnover-limiting oxidative addition (OA).

■ RESULTS AND DISCUSSION

The coupling between cyclohexylamine (**1a**) and methyl 4-bromobenzoate (**2a**) was chosen as a model system for initial optimization of our nucleophile arylation protocol (Table 1). During optimization studies, NiBr$_2$·glyme was identified as the optimal Ni source. Notably, irreproducible results were obtained from batch to batch, likely due to the highly hygroscopic nature of this Ni salt, even when stored in a desiccator. Careful control of the water content was necessary to obtain reproducible results. Storage of the Ni precatalyst in a N$_2$-filled glovebox, together with the addition of 2.5 mol% of water, led to the best results (see Table S1 for more details).

Table 1. Optimized Conditions and Control Experiments[a]

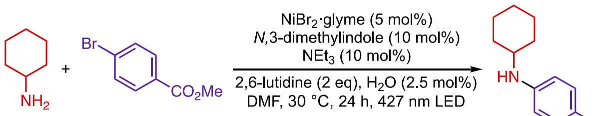

1a **2a** **3a**

entry	other variations	yield of **3a**	remaining ArBr (**2a**)
1	none	79%	21%
2	no NEt$_3$	64%	36%
3	no light	not detected	100%
4	**no *N*,3-dimethylindole**	not detected	100%
5	no NiBr$_2$ glyme	not detected	5% (95% ArH)

[a] Reaction conditions: NiBr$_2$ glyme (0.01 mmol), *N*,3-dimethylindole (0.02 mmol), **1a** (0.4 mmol), **2a** (0.2 mmol), 2,6-lutidine (0.4 mmol), triethylamine (0.02 mmol), H$_2$O (0.005 mmol), and 0.5 mL of DMF. The solution was irradiated with a 427 nm LED and stirred at 30 °C for 24 h. All yields were determined by ^{1}H NMR using 1,3,5-trimethoxybenzene as an internal standard.

The use of a stoichiometric base was observed to increase the reaction yield presumably by preventing protonation of the amine substrate. Mild organic bases were targeted to identify a homogeneous system that facilitates reproducibility and scale up[20] while maintaining a large functional group tolerance. Cost-effective 2,6-lutidine was found to be optimal for this coupling reaction. To our initial surprise, the presence of substoichiometric amounts of triethylamine also led to a yield increase (entries 1 and 2). Lower yields were obtained when triethylamine was used as the sole stoichiometric base (Table S2). The role of the tertiary amine will be revisited later in the manuscript. Finally, the specific stoichiometry, concentration, and temperature parameters were optimized with the help of a Bayesian optimization tool developed by the Doyle lab (entry 1).[21]

Without light or *N*,3-dimethylindole, no coupling product (**3a**) was detected, and the starting materials (**1a** and **2a**) were fully recovered (entries 3 and 4). When Ni was excluded from the reaction conditions, we again saw no coupling product, but in this case, aryl bromide **2a** had been reduced to the corresponding proto-debrominated arene (methyl benzoate; see Figure 4a) in high yields (entry 5). Subsequent control experiments revealed that this debromination reaction requires both *N*,3-dimethylindole and light. The mechanism for the formation of a protonated arene and its relevance for the heteroatom arylation reaction will be discussed in detail in the mechanistic investigation section of this paper.

During the reaction optimization, no amine arylation was detected when methanol was used as the solvent. Instead, complete conversion to the methanol arylation product was observed. Intrigued by this result, we explored whether this reactivity could be extended to other oxygenated nucleophiles. However, directly applying the reaction conditions optimized for cyclohexylamine (**1a**) resulted in no reaction when methanol was used as the substrate.

We hypothesized that the lack of reactivity was due to the absence of a ligand. The addition of the commonly used 4,4′-di-*tert*-butyl-2,2′-dipyridyl (dtbbpy) ligand also failed to promote the reaction. Given that methanol exhibited reactivity in the presence of **1a**, we then tested a mixture of equimolar amounts of **1a** and methanol with DMF as the solvent. Under these conditions, both arylation products were observed in 62% and 14% yields for the alcohol arylation and amine arylation, respectively.

Encouraged by this finding, we screened other amines that could potentially act as ligands while coupling at a slower rate. Ultimately, we identified that *N*-methylcyclohexylamine (Me(Cy)NH) affords optimal reactivity. During the scope exploration, it was observed that the addition of Me(Cy)NH to the reaction conditions greatly increased the reactivity of most substrates (Figure 2).[19] In contrast, no effect on the reaction yield was observed when Me(Cy)NH was added to highly nucleophilic substrates (Figure 3), likely due to competing Ni coordination being more pronounced for highly nucleophilic amines. Kinetic data will be presented to further rationalize the effect of the Me(Cy)NH additive on the reaction mechanism.

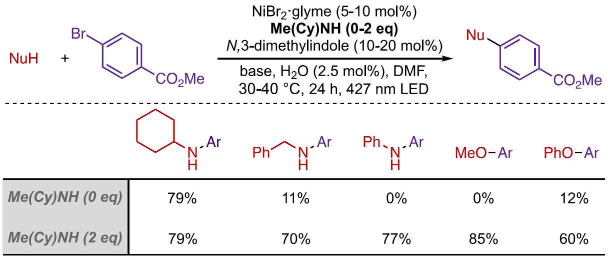

Figure 2. Product yield in the presence and absence of Me(Cy)NH. Reaction conditions for nitrogen nucleophiles: $NiBr_2$·glyme (0.01 mmol), Me(Cy)NH (0.4 or 0 mmol, as indicated), *N*,3-dimethylindole (0.02 mmol), nitrogen nucleophile (0.4 mmol), **2a** (0.2 mmol), 2,6-lutidine (0.4 mmol), triethylamine (0.02 mmol), H_2O (0.005 mmol), and 0.5 mL of DMF. The solution was irradiated with a 427 nm LED and stirred at 30 °C for 24 h. Reaction conditions for oxygen nucleophiles: $NiBr_2$·glyme (0.02 mmol), Me(Cy)NH (0.4 or 0 mmol, as indicated), *N*,3-dimethylindole (0.04 mmol), oxygen nucleophile (0.6 mmol), **2a** (0.2 mmol), H_2O (0.005 mmol), and 0.5 mL of DMF. The solution was irradiated with a 427 nm LED and stirred at 40 °C for 24 h. All yields were determined by ^1H NMR using 1,3,5-trimethoxybenzene as an internal standard.

The scope exploration, depicted in Figure 3, demonstrates the broad applicability of the reaction conditions. A variety of primary amines successfully yielded the desired products, with both alkyl and benzyl amines being well tolerated (**3a**−**3e**). Notably, more challenging α-secondary (**3a** and **3e**) and sterically encumbered (**3b**) substrates were not only compatible but also afforded higher yields compared to simpler linear amines (**3c** and **3d**). The superior performance of this approach with sterically encumbered substrates makes it a valuable complementary strategy to other organometallic methodologies. We believe this trend is rooted in the reaction mechanism, which is discussed in the next section.

Unsurprisingly, highly nucleophilic cyclic secondary amines were well suited for this transformation (**3f**−**3i**). Additionally, less nucleophilic nitrogen-containing groups, such as anilines, amides, and sulfonamides, also underwent arylation in good yields when the reaction was moderately heated to 50 °C (**3j**−**3l**).

A variety of alcohol nucleophiles were also well tolerated, with both electron-rich and electron-poor primary alcohols leading to high product yields (**5a**−**5d**). Cyclic and acyclic secondary alcohols were also amenable to the reaction conditions, albeit displaying more moderate yields of the coupling products (**5e**−**5h**). Phenols exhibited excellent reactivity, affording high yields, regardless of their electronic properties (**5i**−**5k**). Finally, the successful use of water as a nucleophile allowed access to phenol **5l**, further showcasing the versatility of this methodology.

The aryl bromide scope demonstrated consistently high yields across a variety of electronic environments. Likely due to the electron-rich nature of the ligand system, substrates that are traditionally challenging in Ni-catalyzed cross-coupling reactions, such as electron-rich aryl halides, led to high yields in both heteroatom arylation reactions (**3o**−**3r** and **5o**−**5p**, respectively). Notably, even ortho-substituted aromatic rings were well tolerated, as evidenced by the good yields obtained for *o*-methyl and *o*-cyano arenes (**3s** and **3t**).

However, limitations were observed with secondary acyclic amines (similar to our ligand) and substrates containing strongly coordinating groups (e.g., pyridines). Nevertheless, the moderate temperature and mildly basic conditions allowed for excellent functional group tolerance, enabling access to elimination-prone **5h** and the coupling of a highly reactive styrene to yield **5p**. Additionally, we tested the scalability of this coupling protocol by running a 2 mmol scale reaction using the same setup. The final product, **3f**, was isolated in an excellent 90% yield.

Next, we conducted a series of mechanistic experiments, initially focusing on understanding the role of light and indole in enabling this coupling reaction. Building on our initial control experiments (Figure 2, entries 3−5), we aimed to simplify the conditions to better understand the formation of the debrominated arene (**4**). Once again, both light and indole were found to be required to access this reactivity (Figure 4a, entries 1 and 2). The reduction of electron-rich arenes was also observed, albeit in a significantly lower yield (entry 3). And finally, utilizing a stoichiometric amount of indole in the absence of amines, the reduced arene (**4**) was still formed (entry 5).

We first tested whether this light-induced reactivity was driven by the formation of an electron donor−acceptor complex or the direct excitation of the indole. No UV−vis absorption spectral changes were observed for all possible mixtures of the reaction components, discarding the possibility of the formation of electron donor−acceptor complexes (Figure S15). Subsequently, we tested if the direct excitation of the indole (which absorbs at 427 nm) was enabling the aryl halide reduction. Stern−Volmer studies using aryl bromide **2a** as the quencher were conducted. Quenching of the indole emission was observed when irradiating at 420 nm (Figure S17). We rationalized these results as potentially indicative of a photoinduced electron transfer from the excited indole to the aryl bromide that would lead to the formation of aryl radicals. This reactivity is reminiscent of the Witkop cyclization, where upon UV light excitation, indoles undergo single-electron transfer to reduce α-halo carbonyls and render carbon-centered radicals.[22] However, in those reactions, the generated radicals subsequently undergo intramolecular cyclization.

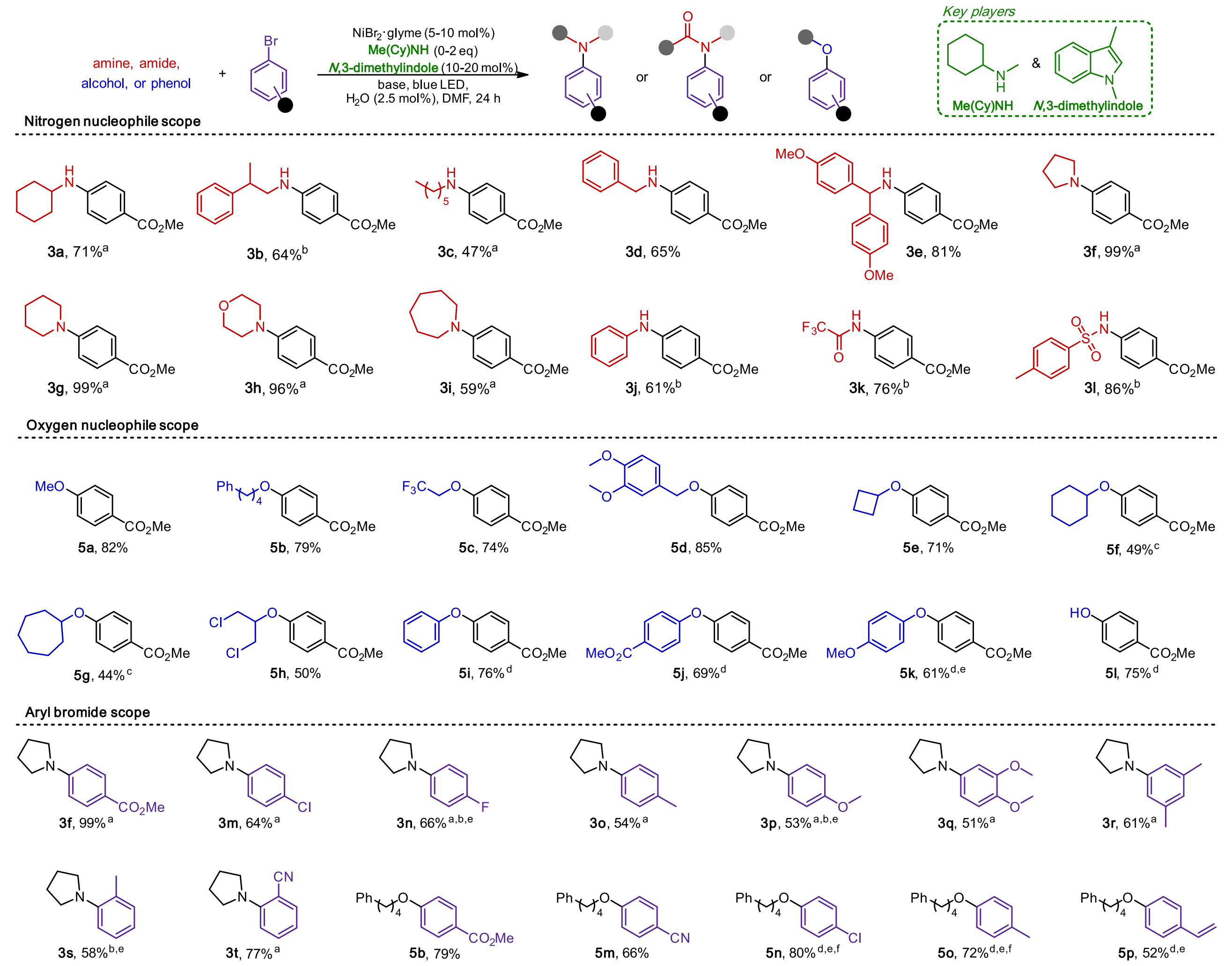

Figure 3. Reaction scope for the indole-mediated Ni-photoredox heteroatom arylation reaction. Reaction conditions for nitrogen nucleophiles: $NiBr_2$·glyme (0.01 mmol), Me(Cy)NH (0.4 or 0 mmol, as indicated), *N*,3-dimethylindole (0.02 mmol), nitrogen nucleophile (0.4 mmol), **2a** (0.2 mmol), 2,6-lutidine (0.4 mmol), triethylamine (0.02 mmol), H_2O (0.005 mmol), and 0.5 mL of DMF. The solution was irradiated with a 427 nm LED and stirred at 30 °C for 24 h. Reaction conditions for oxygen nucleophiles: $NiBr_2$·glyme (0.02 mmol), Me(Cy)NH (0.4 mmol), *N*,3-dimethylindole (0.04 mmol), oxygen nucleophile (0.6 mmol), **2a** (0.2 mmol), H_2O (0.005 mmol), and 0.5 mL of DMF. The solution was irradiated with a 427 nm LED and stirred at 40 °C for 24 h. All yields refer to isolated product **3** or **5** after purification. [a]No Me(Cy)NH was added. [b]Reaction carried out at 50 °C. [c]Yields were determined by ^1H NMR using 1,3,5-trimethoxybenzene as an internal standard. [d]DABCO was added (0.2 mmol). [e]2-methylindole was used instead of *N*,3-dimethylindole. [f]48 h reaction.

The formation of aryl radicals under our visible-light-mediated conditions (Figure 4a, entry 1) was probed utilizing spin trap **5** (Figure 4b). EPR analysis of the reaction crude revealed the addition of a radical species to the spin trap. To further corroborate aryl radical trapping to form **6**, the same trapping experiment was repeated utilizing a previously reported photochemical procedure for generating this aryl radical.[23] The spectral data from both EPR experiments matched (Figures S13 and S14), supporting the formation of aryl radicals under these conditions.

With this information in hand, we hypothesized that upon indole excitation electron transfer to the aryl bromide could occur. Subsequent mesolysis of the reduced arene would generate the aryl radical (Figure 4c). The oxidized indole is also generated as a byproduct of this step; however, no appreciable indole degradation is observed in either the Ni-catalyzed reactions or the control experiments depicted in entries 1 and 3 (Figure 4a).

To test if the amines, either the substrates or the triethylamine additive, served as the terminal reductant for regenerating the neutral indole, control experiments for the aryl halide reduction in the absence of the amines were conducted. In the absence of amines and with a catalytic amount of indole, complete degradation of the indole was observed together with no reduced arene formation (Figure 4a, entry 4). When using stoichiometric amounts of *N*,3-dimethyl indole, the dehalogenated product **4** was observed in a 24% yield, with 46% of the starting indole remaining unreacted (Figure 4a, entry 5). We were unsuccessful in characterizing the degradation byproducts derived from indole, which are not detected in the crude ^1H NMR. These results suggest that the indole radical cation may be reduced by the amines in solution, thereby preventing indole degradation during the catalytic cross-coupling reactions (Figure 4c). Triethylamine has a milder oxidation potential than *N*,3-dimethylindole and the amine substrates[24] and is therefore proposed to act preferentially as the terminal reductant.

a) Control experiments for ArH (4) formation

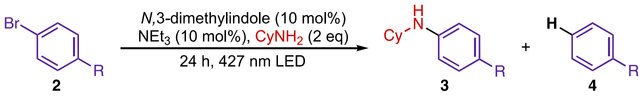

Entry	*Aryl bromide (2)*	*Other variations*	*Yield of 3*	*Yield of 4*
1	R = CO_2Me	None	Not detected	95%
2	R = CO_2Me	No light or no indole	Not detected	Not detected
3	R = OMe	None	Not detected	8%
4	R = CO_2Me	excluding NEt_3 and $CyNH_2$	Not detected	Not detected
5	R = CO_2Me	*N*,3-dimethylindole (1 eq) excluding NEt_3 and $CyNH_2$	Not detected	24%

b) Probing aryl radical formation

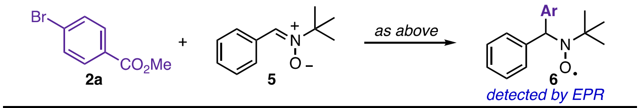

c) Proposed mechanism

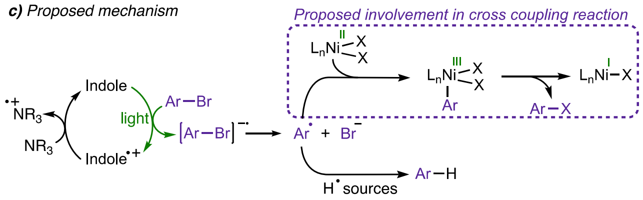

Figure 4. Probing the aryl proto debromination mechanism. (a) Reaction conditions: **2** (0.2 mmol), cyclohexylamine (0.4 mmol), *N*,3-dimethylindole (0.02 mmol), triethylamine (0.02 mmol), and 0.5 mL of DMF. The solution was irradiated with a 427 nm LED and stirred at 30 °C for 24 h. All yields were determined by ^{1}H NMR using 1,3,5-trimethoxybenzene as an internal standard. (b) Reaction conditions: **2a** (0.2 mmol), 5 (0.6 mmol), cyclohexylamine (0.2 mmol), *N*,3-dimethylindole (0.02 mmol), and 3 mL of C_6H_6. The solution was irradiated with a 427 nm LED at room temperature for 24 h. The reaction crude was analyzed by EPR spectroscopy at room temperature.

Most Ni-photoredox heteroatom arylation reactions have been shown to be initiated by the reduction of Ni(II) complexes.[2c,6,18,25] A similar mechanism could be envisioned to be operative under our catalytic conditions, where a photoinduced electron transfer from indole may reduce the Ni(II) complexes. Stern−Volmer quenching experiments were not feasible to study this hypothesis given the strong absorption of the Ni complexes across the indole excitation region (Figures S15 and S16). This pathway was investigated by EPR analysis of irradiated mixtures of *N*,3-dimethylindole and $NiBr_2$·glyme in the absence or presence of the amine partners. No Ni(I) characteristic signals were observed by EPR at 77 K in any of these trials. This suggests that the photochemical steps may not be related to a direct reduction of Ni(II) by excited indoles, which led us to consider alternative pathways for the reduction of Ni(II) to Ni(I). We wondered whether the previously discussed aryl radical formation could be involved in this step. Ni(II) complexes are known to readily trap radicals to yield intermediates that quickly undergo reductive elimination (Figure 4c).[6c,26] Specifically, Ni(III) complexes have been shown to undergo reductive elimination of aryl halides to yield a Ni(I) halide complex, which can then start catalysis.[27]

We envisioned that kinetic studies would help us decipher whether the aryl radical formation can initiate Ni catalysis. For a mechanism where the aryl bromide is involved only in the cross-coupling catalytic cycle, a maximum of a first order with respect to aryl bromide would be expected. In this case, no more than one molecule of aryl bromide would be involved in or prior to the turnover-limiting step. However, if the aryl bromide is involved both in the Ni catalytic cycle (chain propagation) and in Ni reduction (which serves as initiation to the radical chain), one could envision measuring an order larger than one with respect to the aryl bromide. Such a value would implicate the involvement of the aryl bromide in multiple stages of the mechanism.

Initial rate kinetic measurements revealed a greater than first order dependence (order = 1.5) in aryl bromide (Figures S1 and S2). This is suggestive of its involvement in both the initiation and catalytic cycles, which is not compatible with a catalytic cycle where the aryl bromide is involved only in the oxidative addition step. Indeed, one would expect a lesser effect on the reaction rate when increasing the aryl bromide concentration if the photoinduced electron transfer to Ni were operative, as **2** would compete with Ni(II) for the photoinduced electron transfer from indole. These kinetic data therefore provide strong evidence to support the initiation mechanism depicted in Figure 4c.

Besides this aryl bromide dependence, the rate law also includes a fractional order with respect to both amine and *N*,3-dimethylindole and a negative dependence in Ni (order = −0.5). No rate changes were observed when varying the concentration of the base, triethylamine, and water (Figures S1−S10). Unlike the order in aryl bromide, the remainder of the rate law could be compatible with either initiation sequence.

To better understand the origins of the negative order with respect to Ni, we investigated if this was also the case for the reactions with added Me(Cy)NH. As shown in Figure 5, a completely different kinetic behavior is observed for a reaction containing the secondary amine additive, which now shows a positive order (0.6) in Ni.

Deleterious effects of a high Ni loading in Ni-photoredox C−heteroatom couplings have been previously reported. This behavior has been consistently attributed to pervasive side reactions that are bimolecular in Ni and lead to the formation of off-cycle species. Specifically, comproportionation between Ni(I) and Ni(III) species, as well as disproportionation or dimerization of Ni(I) complexes, have been proposed as key deactivation pathways.[2c,6,18] In this context, we hypothesize that the sterically encumbered nature of the amine used here inhibits the formation of the bimetallic transition states required for these off-cycle processes. The improved yields observed for sterically hindered substrates (Figure 3) further support this rationale.

As previously discussed, the large rate dependence (1.5 order) on aryl bromide supports the presence of a radical chain mechanism. This is also in line with prior mechanistic studies of Ni-photoredox C(sp^2)−heteroatom coupling reactions.[2c,6,18,25] Resultingly, a Ni(I/III) catalytic cycle, initiated by the formation of aryl radicals, is proposed (Figure 6).This mechanistic manifold is also supported by the observed rate order with respect to Ni. The productive catalytic cycle (presumably first order in Ni) competes with undesired pathways that are second order in Ni and lead to the formation of off-cycle Ni(0), Ni(II), and/or bimetallic species (gray arrows). This results in the increased sequestering of Ni off-cycle at higher Ni loadings, which has been shown to lead to orders lower than 1, and in some cases negative, with respect to Ni.[2c,6,25]

https://doi.org/10.1021/acscatal.5c03251
ACS Catal. 2025, 15, 10760−10767

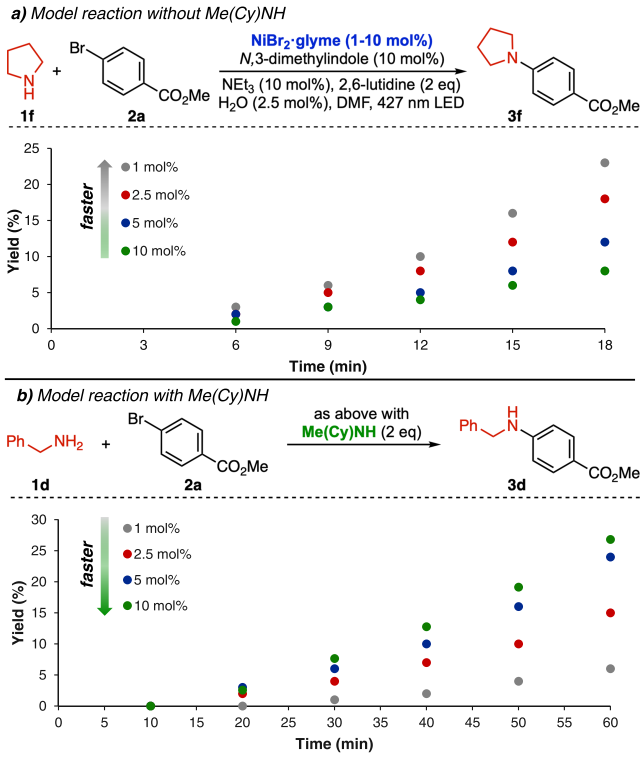

Figure 5. Effect of Ni loading on the reaction rate. Reaction conditions: $NiBr_2$·glyme (0.002–0.02 mmol), Me(Cy)NH (0.4 or 0 mmol, as indicated), *N*,3-dimethylindole (0.02 mmol), nitrogen nucleophile **1** (0.4 mmol), **2a** (0.2 mmol), 2,6-lutidine (0.4 mmol), triethylamine (0.02 mmol), H_2O (0.005 mmol), and 0.5 mL of DMF. The solution was irradiated with a 427 nm LED and stirred for the indicated time. Yields were determined by ^1H NMR.

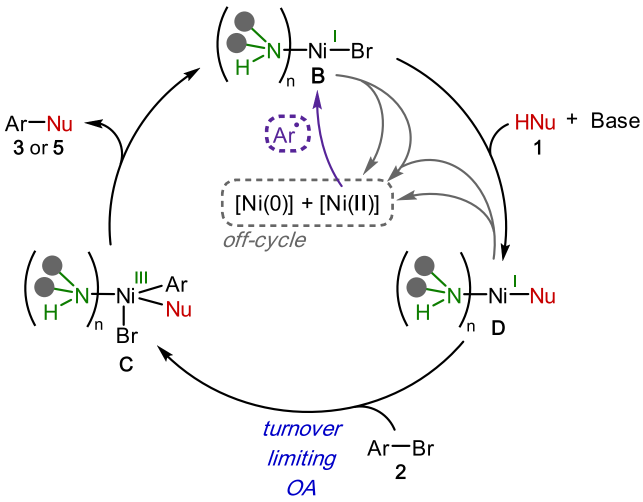

Figure 6. Proposed mechanism.

The catalytic cycle starts with the formation of the Ni(I) bromide complex **B**. Subsequent ligand exchange and turnover-limiting oxidative addition (Figure 6, **D** → **C**) yield the key Ni(III) intermediate **C**. This is proposed to be the slow step of the reaction, as the rate law includes amine, Ni, and aryl bromide concentrations. It is hypothesized that Me(Cy)NH was found to be the optimal additive because it serves as an electron-rich ligand that can accelerate the rate-limiting oxidative addition step while hampering bimetallic side reactions (depicted in gray). Highly nucleophilic substrates likely outcompete Me(Cy)NH for coordination to Ni, thereby diminishing its contribution to the catalysis. Finally, stoichiometric experiments in related systems have demonstrated the final reductive elimination step to be fast.[5]

CONCLUSION

In summary, we have developed a Ni-catalyzed C—N and C—O coupling protocol that is mediated by visible light and eliminates the need for costly designer photocatalysts or ligands. This methodology accommodates a broad range of coupling partners and exhibits complementary reactivity to existing systems, achieving high yields, even for sterically encumbered and electron-rich substrates. Key to this reactivity was the discovery that indoles can facilitate these reactions through light-driven aryl radical formation, a rare initiation mechanism for activating Ni(II) off-cycle species. Here, the indole photocatalyst operates by generating aryl radicals that are trapped to funnel Ni(II) complexes back into the productive Ni(I/III) cycle (Figure 6, purple arrows). The data depicted in Figure 4 and the 1.5 order with respect to aryl bromide strongly suggest that aryl radicals are formed under these conditions and that they are relevant to the initiation mechanism. Even electron-rich aryl halides were demonstrated to be amenable to photoreduction to generate sufficient aryl radicals for initiating high yielding coupling reactions (Figure 4a, entry 4). The compatibility of this indole-mediated aryl radical formation manifold with organometallic catalysis is expected to enable a broader range of synthetic methodologies beyond Ni-mediated processes.

Finally, we have uncovered a divergence from the mechanisms proposed in previous studies, where Ir photocatalysts are required to reduce off-cycle Ni(II) species.[2c,6,25] We have also introduced the use of secondary amines as optimal ligands for this Ni-photoredox process and presented preliminary kinetic data highlighting their ability to suppress undesired pathways that funnel Ni off-cycle. Rigorous investigations into the speciation of amine-ligated Ni complexes and photochemical studies of indole-mediated electron transfer are ongoing efforts in our laboratory to further understand this reactivity.

METHODS

In a N_2-filled glovebox, $NiBr_2$·glyme (31 mg, 0.1 mmol) was added to a dram vial. The dram vial was then capped with a PTFE/Silicone vial septum and electrical taped. After the dram vial containing $NiBr_2$·glyme was transported out of the glovebox, a needle connected to a N_2 gas flow was inserted into the dram vial through the PTFE/Silicone septa to ensure the vial was under positive N_2 pressure. 5 mL of dimethylformamide (DMF) from an SPS solvent system was added into the dram vial. Subsequently, H_2O (0.9 μL, 0.05 mmol) was added to the solution. 0.5 mL of this solution was then added to an oven-dried 10 mL Schlenk tube charged with a magnetic stir bar and capped with a ground glass stopper that was kept under N_2. This was followed by the addition of N,3-dimethylindole (2.8 μL, 0.02 mmol), NEt_3 (2.8 μL, 0.02 mmol), and 2,6-lutidine (46 μL, 0.4 mmol). The reaction vessel was then allowed to stir for 5 min at room temperature before the addition of aryl bromide (0.2 mmol) and amine (0.4 mmol). It must be noted that the order of addition is imperative. Solid reagents were added to the Schlenk tube via a paper cone while liquid reagents were added via a Hamilton syringe, both under a constant flow of N_2 gas. The ground glass stopper was coated in vacuum grease before sealing the reaction vessel, and the stopper was subsequently wrapped in parafilm. The reaction vessel was placed 1 in. in front of a 427 nm Kessil LED lamp while being submerged in a temperature-controlled water bath in a crystallizing dish held at a constant temperature.

Upon completion, the reaction mixture was filtered through a pad of Celite using dichloromethane or ethyl acetate. The crude filtrate was concentrated in vacuo and adsorbed onto a small amount of silica. This material was loaded onto a chromatography column, and the desired product was isolated.

■ ASSOCIATED CONTENT

SI Supporting Information

The Supporting Information is available free of charge at https://pubs.acs.org/doi/10.1021/acscatal.5c03251.

> All additional experimental details, materials, nitrogen nucleophile arylation optimization, mechanistic studies, synthetic procedures, and ^{1}H, ^{13}C, and ^{19}F NMR characterization of the products (PDF)

■ AUTHOR INFORMATION

Corresponding Author

Ana Bahamonde − *Department of Chemistry, University of California, Riverside, California 92521, United States;* orcid.org/0000-0002-7713-1901;
Email: ana.bahamonde@ucr.edu

Authors

Harsh P. Chavda − *Department of Chemistry, University of California, Riverside, California 92521, United States;* orcid.org/0009-0009-8924-694X
Kevin J. Liang − *Department of Chemistry, University of California, Riverside, California 92521, United States*
Tanner J. Megna − *Department of Chemistry, University of California, Riverside, California 92521, United States*
Olivia R. Taylor − *Department of Chemistry, University of California, Riverside, California 92521, United States;* orcid.org/0000-0002-5542-7568
Grace Kim − *Department of Chemistry, University of California, Riverside, California 92521, United States*
Angie L. López − *Department of Chemistry, University of California, Riverside, California 92521, United States*

Complete contact information is available at:
https://pubs.acs.org/10.1021/acscatal.5c03251

Author Contributions

The manuscript was written through contributions of all authors.

Notes

The authors declare no competing financial interest.

■ ACKNOWLEDGMENTS

This work was supported by the NIH (R35GM154874-01) and the University of California, Riverside.

■ REFERENCES

(1) (a) Corcoran, E. B.; Pirnot, M. T.; Lin, S.; Dreher, S. D.; DiRocco, D. A.; Davies, I. W.; Buchwald, S. L.; MacMillan, D. W. Aryl amination using ligand-free Ni (II) salts and photoredox catalysis. *Science* **2016**, *353*, 279−283. (b) Welin, E. R.; Le, C.; Arias-Rotondo, D. M.; McCusker, J. K.; MacMillan, D. W. Photosensitized, energy transfer-mediated organometallic catalysis through electronically excited nickel (II). *Science* **2017**, *355*, 380−385. (c) Terrett, J. A.; Cuthbertson, J. D.; Shurtleff, V. W.; MacMillan, D. W. Switching on elusive organometallic mechanisms with photoredox catalysis. *Nature* **2015**, *524*, 330−334.

(2) (a) Zhu, C.; Yue, H.; Jia, J.; Rueping, M. Recent Advances in Nickel-Catalyzed C-Heteroatom Cross-Coupling Reactions under Mild Conditions via Facilitated Reductive Elimination. *Angew. Chem. Int. Ed.* **2021**, *60*, 17810−17831. (b) Zhu, S.; Li, H.; Li, Y.; Huang, Z.; Chu, L. Exploring visible light for carbon−nitrogen and carbon−oxygen bond formation via nickel catalysis. *Org. Chem. Front.* **2023**, *10*, 548−569. (c) Taylor, O. R.; Saucedo, P. J.; Bahamonde, A. Leveraging the Redox Promiscuity of Nickel To Catalyze C−N Coupling Reactions. *J. Org. Chem.* **2024**, *89*, 16093−16105.

(3) (a) Lavoie, C. M.; MacQueen, P. M.; Rotta-Loria, N. L.; Sawatzky, R. S.; Borzenko, A.; Chisholm, A. J.; Hargreaves, B. K.; McDonald, R.; Ferguson, M. J.; Stradiotto, M. Challenging nickel-catalysed amine arylations enabled by tailored ancillary ligand design. *Nat. Commun.* **2016**, *7*, 11073. (b) Morrison, K. M.; Stradiotto, M. The development of cage phosphine 'DalPhos' ligands to enable nickel-catalyzed cross-couplings of (hetero) aryl electrophiles. *Chem. Sci.* **2024**, *15*, 7394−7407. (c) Ruiz-Castillo, P.; Buchwald, S. L. Applications of palladium-catalyzed C−N cross-coupling reactions. *Chem. Rev.* **2016**, *116*, 12564−12649. (d) Ley, S. V.; Thomas, A. W. Modern Synthetic Methods for Copper-Mediated C (aryl)-O, C (aryl)-N, and C (aryl)-S Bond Formation. *Angew. Chem., Int. Ed.* **2003**, *42*, 5400−5449. (e) Dorel, R.; Grugel, C. P.; Haydl, A. M. The Buchwald−Hartwig amination after 25 years. *Angew. Chem., Int. Ed.* **2019**, *58*, 17118−17129.

(4) (a) Goldschmid, S. L.; Soon Tay, N. E.; Joe, C. L.; Lainhart, B. C.; Sherwood, T. C.; Simmons, E. M.; Sezen-Edmonds, M.; Rovis, T. Overcoming Photochemical Limitations in Metallaphotoredox Catalysis: Red-Light-Driven C−N Cross-Coupling. *J. Am. Chem. Soc.* **2022**, *144*, 22409−22415. (b) Konev, M. O.; McTeague, T. A.; Johannes, J. W. Nickel-catalyzed photoredox-mediated cross-coupling of aryl electrophiles and aryl azides. *ACS Catal.* **2018**, *8*, 9120−9124.

(5) (a) Han, R.; Hillhouse, G. L. Carbon− oxygen reductive-elimination from nickel (II) oxametallacycles and factors that control formation of ether, aldehyde, alcohol, or ester products. *J. Am. Chem. Soc.* **1997**, *119*, 8135−8136. (b) Koo, K.; Hillhouse, G. L. Carbon-nitrogen bond formation by reductive elimination from nickel (II) amido alkyl complexes. *Organometallics* **1995**, *14*, 4421−4423. (c) Koo, K.; Hillhouse, G. L. Indoline Synthesis via Coupling of Phenethyl Grignard Reagents with Organoazides Mediated by (Alkylphosphine) nickel (II) Complexes. *Organometallics* **1996**, *15*, 2669−2671. (d) Lin, B. L.; Clough, C. R.; Hillhouse, G. L. Interactions of aziridines with nickel complexes: oxidative-addition and reductive-elimination reactions that break and make C− N bonds. *J. Am. Chem. Soc.* **2002**, *124*, 2890−2891.

(6) (a) Sun, R.; Qin, Y.; Ruccolo, S.; Schnedermann, C.; Costentin, C.; Nocera, D. G. Elucidation of a Redox-Mediated Reaction Cycle for Nickel-Catalyzed Cross Coupling. *J. Am. Chem. Soc.* **2019**, *141*, 89−93. (b) Till, N. A.; Tian, L.; Dong, Z.; Scholes, G. D.; MacMillan, D. W. Mechanistic Analysis of Metallaphotoredox C−N Coupling: Photocatalysis Initiates and Perpetuates Ni (I)/Ni (III) Coupling Activity. *J. Am. Chem. Soc.* **2020**, *142*, 15830−15841. (c) Cagan, D. A.; Bím, D.; Kazmierczak, N. P.; Hadt, R. G. Mechanisms of Photoredox Catalysis Featuring Nickel−Bipyridine Complexes. *ACS Catal.* **2024**, *14*, 9055−9076.

(7) (a) Du, Y.; Pearson, R. M.; Lim, C. H.; Sartor, S. M.; Ryan, M. D.; Yang, H.; Damrauer, N. H.; Miyake, G. M. Strongly reducing, visible-light organic photoredox catalysts as sustainable alternatives to precious metals. *Chem.—Eur. J.* **2017**, *23*, 10962−10968. (b) Kudisch, M.; Lim, C.-H.; Thordarson, P.; Miyake, G. M. Energy transfer to Ni-amine complexes in dual catalytic, light-driven C−N cross-coupling reactions. *J. Am. Chem. Soc.* **2019**, *141*, 19479−19486. (c) Lu, J.; Pattengale, B.; Liu, Q.; Yang, S.; Shi, W.; Li, S.; Huang, J.; Zhang, J. Donor−acceptor fluorophores for energy-transfer-mediated photo-

catalysis. *J. Am. Chem. Soc.* **2018**, *140*, 13719−13725. (d) Yang, L.; Huang, Z.; Li, G.; Zhang, W.; Cao, R.; Wang, C.; Xiao, J.; Xue, D. Synthesis of phenols: organophotoredox/nickel dual catalytic hydroxylation of aryl halides with water. *Angew. Chem., Int. Ed.* **2018**, *57*, 1968−1972.

(8) (a) Sun, R.; Qin, Y.; Nocera, D. G. General Paradigm in Photoredox Nickel-Catalyzed Cross-Coupling Allows for Light-Free Access to Reactivity. *Angew. Chem.* **2020**, *132*, 9614−9620. (b) Saeb, R.; Boulenger, B.; Cornella, J. "Naked Nickel"-Catalyzed Amination of Heteroaryl Bromides. *Org. Lett.* **2024**, *26*, 5928−5933.

(9) (a) Li, C.; Kawamata, Y.; Nakamura, H.; Vantourout, J. C.; Liu, Z.; Hou, Q.; Bao, D.; Starr, J. T.; Chen, J.; Yan, M.; et al. Electrochemically enabled, nickel-catalyzed amination. *Angew. Chem., Int. Ed.* **2017**, *56*, 13088. (b) Kawamata, Y.; Vantourout, J. C.; Hickey, D. P.; Bai, P.; Chen, L.; Hou, Q.; Qiao, W.; Barman, K.; Edwards, M. A.; Garrido-Castro, A. F.; deGruyter, J. N.; Nakamura, H.; Knouse, K.; Qin, C.; Clay, K. J.; Bao, D.; Li, C.; Starr, J. T.; Garcia-Irizarry, C.; Sach, N.; White, H. S.; Neurock, M.; Minteer, S. D.; Baran, P. S. Electrochemically Driven, Ni-Catalyzed Aryl Amination: Scope, Mechanism, and Applications. *J. Am. Chem. Soc.* **2019**, *141*, 6392−6402.

(10) (a) Song, G.; Nong, D.-Z.; Li, J.-S.; Li, G.; Zhang, W.; Cao, R.; Wang, C.; Xiao, J.; Xue, D. General method for the amination of aryl halides with primary and secondary alkyl amines via nickel photocatalysis. *J. Org. Chem.* **2022**, *87*, 10285−10297. (b) Lim, C.-H.; Kudisch, M.; Liu, B.; Miyake, G. M. C−N cross-coupling via photoexcitation of nickel−amine complexes. *J. Am. Chem. Soc.* **2018**, *140*, 7667−7673.

(11) (a) Li, J.; Huang, C.-Y.; Li, C.-J. Two-in-one metallaphotoredox cross-couplings enabled by a photoactive ligand. *Chem.* **2022**, *8*, 2419−2431. (b) Cavedon, C.; Gisbertz, S.; Reischauer, S.; Vogl, S.; Sperlich, E.; Burke, J. H.; Wallick, R. F.; Schrottke, S.; Hsu, W. H.; Anghileri, L.; et al. Intraligand charge transfer enables visible-light-mediated nickel-catalyzed cross-coupling reactions. *Angew. Chem.* **2022**, *134*, No. e202211433.

(12) Li, J.; Wang, P.; Bai, B.; Xiao, Y.; Wan, Y.-F.; Yan, Y.; Li, F.; Song, G.; Li, G.; Wang, C.; Xue, D.; et al. Synthesis, Characterization, and Catalytic Activity of Ni (0)(DQ) dtbbpy, an Air-Stable, Bifunctional Red-Light-Sensitive Precatalyst. *J. Am. Chem. Soc.* **2025**, *147*, 5851−5859.

(13) Ting, S. I.; Garakyaraghi, S.; Taliaferro, C. M.; Shields, B. J.; Scholes, G. D.; Castellano, F. N.; Doyle, A. G. 3d-d excited states of Ni (II) complexes relevant to photoredox catalysis: spectroscopic identification and mechanistic implications. *J. Am. Chem. Soc.* **2020**, *142*, 5800−5810.

(14) Ni, S.; Halder, R.; Ahmadli, D.; Reijerse, E. J.; Cornella, J.; Ritter, T. C−heteroatom coupling with electron-rich aryls enabled by nickel catalysis and light. *Nat. Catal.* **2024**, *7*, 733−741.

(15) (a) Luo, H.; Wang, G.; Feng, Y.; Zheng, W.; Kong, L.; Ma, Y.; Matsunaga, S.; Lin, L. Photoinduced Nickel-Catalyzed Carbon−Heteroatom Coupling. *Chem.—Eur. J.* **2023**, *29*, No. e202202385. (b) Feng, Y.; Luo, H.; Yu, F.; Liao, Q.; Lin, L. Sodium-iodide-promoted nickel-catalyzed C−N cross-coupling of aryl chlorides and N-nucleophiles under visible-light irradiation. *Green Chem.* **2023**, *25*, 2361−2367.

(16) Na, H.; Mirica, L. M. Deciphering the mechanism of the Ni-photocatalyzed C−O cross-coupling reaction using a tridentate pyridinophane ligand. *Nat. Commun.* **2022**, *13*, 1313.

(17) Bahri, J.; Deolka, S.; Vardhanapu, P. K.; Khaskin, E.; Govindarajan, R.; Fayzullin, R. R.; Vasylevskyi, S.; Khusnutdinova, J. R. Photoinduced Carbon− Heteroatom Cross-Coupling Catalyzed by Nickel Naphthyridine Complexes. *Chem. Catal. Chem.* **2023**, *15*, No. e202301142.

(18) Liang, K. J.; Taylor, O. R.; López, A. L.; Woo, R. J.; Bahamonde, A. Indole Nucleophile Triggers Mechanistic Divergence in Ni-Photoredox N-Arylation. *Chem.—Eur. J.* **2024**, *30*, No. e202402524.

(19) (a) Düker, J.; Philipp, M.; Lentner, T.; Cadge, J. A.; Lavarda, J. E.; Gschwind, R. M.; Sigman, M. S.; Ghosh, I.; König, B. Cross-coupling reactions with nickel, visible light, and tert-butylamine as a bifunctional additive. *ACS Catal.* **2025**, *15*, 817−827. (b) Ghosh, I.; Shlapakov, N.; Karl, T. A.; Düker, J.; Nikitin, M.; Burykina, J. V.; Ananikov, V. P.; König, B. General cross-coupling reactions with adaptive dynamic homogeneous catalysis. *Nature* **2023**, *619*, 87−93.

(20) (a) Falß, S.; Tomaiuolo, G.; Perazzo, A.; Hodgson, P.; Yaseneva, P.; Zakrzewski, J.; Guido, S.; Lapkin, A.; Woodward, R.; Meadows, R. E. A continuous process for Buchwald−Hartwig amination at micro-, lab-, and mesoscale using a novel reactor concept. *Org. Process Res. Dev.* **2016**, *20*, 558−567. (b) Yang, J. C.; Niu, D.; Buchwald, S. Use of a catalytic co-solvent, N, N-dimethyl octanamide, allows the flow synthesis of Gleevec with no solvent switch. *Angew. Chem., Int. Ed.* **2016**, *55*, 2531.

(21) (a) Torres, J. A. G.; Lau, S. H.; Anchuri, P.; Stevens, J. M.; Tabora, J. E.; Li, J.; Borovika, A.; Adams, R. P.; Doyle, A. G. A multi-objective active learning platform and web app for reaction optimization. *J. Am. Chem. Soc.* **2022**, *144*, 19999−20007. (b) Shields, B. J.; Stevens, J.; Li, J.; Parasram, M.; Damani, F.; Alvarado, J. I. M.; Janey, J. M.; Adams, R. P.; Doyle, A. G. Bayesian reaction optimization as a tool for chemical synthesis. *Nature* **2021**, *590*, 89−96.

(22) (a) Hammond, G. S.; McCall, M.; Yonemitsu, O.; Witkop, B. Mechanisms of photochemical reactions in solution. LXV. Quenching of excited singlet states of electron-rich aromatic compounds by methyl chloroacetate. *J. Am. Chem. Soc.* **1970**, *92*, 6991−6993. (b) Gritsch, P. J.; Leitner, C.; Pfaffenbach, M.; Gaich, T. The Witkop Cyclization: A Photoinduced C- H Activation of the Indole System. *Angew. Chem., Int. Ed.* **2014**, *53*, 1208−1217.

(23) Devery, J. J., III; Nguyen, J. D.; Dai, C.; Stephenson, C. R. Light-mediated reductive debromination of unactivated alkyl and aryl bromides. *ACS Catal.* **2016**, *6*, 5962−5967.

(24) Zhou, W.; Chen, X.; Lu, L.; Song, X.-R.; Luo, M.-J.; Xiao, Q. Recent advances in electrocatalytic generation of indole-derived radical cations and their applications in organic synthesis. *Chin. Chem. Lett.* **2024**, *35*, 108902.

(25) Bradley, R. D.; McManus, B. D.; Yam, J. G.; Carta, V.; Bahamonde, A. Mechanistic evidence of a Ni (0/II/III) cycle for nickel photoredox amide arylation. *Angew. Chem., Int. Ed.* **2023**, *62*, No. e202310753.

(26) (a) Diccianni, J. B.; Diao, T. Mechanisms of nickel-catalyzed cross-coupling reactions. *Trends Chem.* **2019**, *1*, 830−844. (b) Lipp, A.; Badir, S. O.; Molander, G. A. Stereoinduction in metallaphotoredox catalysis. *Angew. Chem., Int. Ed.* **2021**, *60*, 1714−1726.

(27) Feng, Y.; Luo, H.; Zheng, W.; Matsunaga, S.; Lin, L. Light-promoted nickel-catalyzed aromatic halogen exchange. *ACS Catal.* **2022**, *12*, 11089−11096.